Multicolor Imaging of Ca^{2+} and Protein Kinase C Signals Using Novel Epifluorescence Microscopy

Asako Sawano,*† Hiroshi Hama,* Naoaki Saito,‡ and Atsushi Miyawaki*

*Laboratory for Cell Function and Dynamics, Advanced Technology Development Center, Brain Science Institute, RIKEN, 2-1 Hirosawa, Wako-city, Saitama, 351-0198, Japan; †Brain Science Research Division, Brain Science and Life Technology Research Foundation, 1-28-12 Narimasu, Itabashi, Tokyo, 175-0094, Japan; and ‡Laboratory of Molecular Pharmacology, Biosignal Research Center, Kobe University, 1-1 Rokkodai-cho, Nada-ku, Kobe, 657-8501, Japan

ABSTRACT Dynamic changes in intracellular free Ca^{2+} concentrations ($[Ca^{2+}]_i$s) control many important cellular events, including binding of Ca^{2+}-calmodulin (Ca^{2+}-CaM) and phosphorylation by protein kinase C (PKC). The two signals compete for the same domains in certain substrates, such as myristoylated alanine-rich PKC-substrate (MARCKS). To observe the convergence and relative time of arrival of CaM and PKC signals at their shared domain of MARCKS, we need to image cells that are loaded with more than two fluorescent dyes at a reasonable speed. We have developed a simple and powerful multicolor imaging system using conventional fluorescence microscopy. The epifluorescence configuration uses a glass reflector and rotating filter wheels for excitation and emission paths. As it is free of dichroic (multichroic) mirrors, multiple fluorescence images can be acquired rapidly regardless of the colors of fluorophores. We visualized Ca^{2+}-CaM and PKC together with the dynamics of their common target, MARCKS, in single live cells. Receptor-activation resulted in translocation of MARCKS from the plasma membrane to cytosol through its phosphorylation by PKC. By observing fluorescence resonance energy transfer, we also obtained direct evidence that Ca^{2+}-CaM binds MARCKS to drag it away from the membrane in circumstances when Ca^{2+}-mobilization predominates over PKC activation.

INTRODUCTION

Many important cellular events that occur on the order of seconds are controlled by dynamic changes in the concentration of intracellular free Ca^{2+} ($[Ca^{2+}]_i$). Therefore, the simultaneous observation of Ca^{2+}-related events and Ca^{2+} dynamics in cells loaded with two or more fluorescent dyes requires that the wavelength be rapidly changed. The optical path of an epifluorescence microscope normally contains both an excitation and an emission filters as well as a dichroic mirror. Although the excitation and the emission filters can be changed automatically and rapidly with rotating filter wheels, the rapid exchange of dichroic mirrors is not common, sometimes resulting in the imperfect registration of the two images. For multi- (dual-) color imaging, the following two reflectors have been commonly used. 1) A long pass dichroic mirror with extended reflection (e.g., 505DRLPXR, Omega) allows the simultaneous observation of $[Ca^{2+}]_i$ (reported by fura-2) and the fluorescence of green fluorescent protein (GFP). The use of this system requires one of the dyes to have a large Stoke's shift. 2) A multichroic mirror allows rapid sequential or completely simultaneous acquisition of multiple images. Such a specialized mirror is very expensive, however, and may only be used with a limited set of dyes. Also, fluorescence detection cannot be fully maximized for a given dye, when its emission spectrum overlaps the adjacent reflective band for the excitation of another dye of longer wavelength.

Due to such equipment-specific limitations, multicolor imaging has not yet gained popularity, although it has been appealing to molecular- and cell-biologists since spectral variants of fluorescent proteins emerged.

Here we describe a simple and powerful imaging system that allows observation of more than two events with a high temporal resolution. As the reflector, the epiilluminating system uses a normal glass plate, which displays a high transmittance. Our system is based on the fact that quantitative fluorescence imaging of live cells requires 1) a minimization of illumination intensity to limit the photodamage of cell samples and photobleaching of dyes and 2) a high efficiency for collecting emitted fluorescence signals to increase the signal-to-noise ratio of images.

Using this system, in the present study, we investigated the complex interplay between Ca^{2+} and protein kinase C (PKC) signals. We visualized Ca^{2+}-calmodulin (Ca^{2+}-CaM) and PKC, together with the redistribution of their common target, the myristoylated alanine-rich PKC substrate (MARCKS), in single live HeLa cells. MARCKS is one of the predominant PKC substrates present in many cell types (for review, see Blackshear, 1993). MARCKS binds to the plasma membrane through both the insertion of the hydrophobic myristate chain into the lipid bilayer and the electrostatic interaction of basic residues from the effector domain with acidic phospholipids. Phosphorylation of MARCKS by PKC introduces negative charges into the basic cluster, reducing the electrostatic interaction with acidic lipids. In many cell types, this results in the translocation of MARCKS from the membrane to the cytoplasm (Kim et al., 1994; Ohmori et al., 2000). Binding of a

Submitted June 19, 2001 and accepted for publication October 30, 2001.

Address reprint requests to Atsushi Miyawaki, Laboratory for Cell Function and Dynamics, Advanced Technology Development Center, Brain Science Institute, RIKEN, 2-1 Hirosawa, Wako-city, Saitama, 351-0198, Japan. Tel.: 81-48-467-5917; Fax: 81-48-467-5924; E-mail: matsushi@brain.riken.go.jp.

0006-3495/02/02/1076/10 $2.00

Ca^{2+}-CaM complex to the basic effector domain also induces translocation from the membrane (Kim et al., 1994), although there has been no reported in situ observation of the complex formation between MARCKS and Ca^{2+}-CaM. PKC and Ca^{2+}-CaM may compete for the effector domain of MARCKS (Graff et al., 1989; Chakravarthy et al., 1995a, 1995b, 1999), regulating its phosphorylation state. If so, a surge of Ca^{2+}-CaM complexes would bind to membrane-associated MARCKS, rendering the phosphorylation sites in the effector domain inaccessible to PKC. Conversely, the phosphorylation of MARCKS by PKC could eliminate the protein's affinity for Ca^{2+}-CaM. In both cases, MARCKS is released from the plasma membrane.

To observe the convergence and the relative time taken by the two signals (Ca^{2+}-CaM and PKC) to interact with membrane-associated MARCKS, which is then redistributed to the cytosol, a 3-fluorophore imaging system is required. Furthermore, we extended the epiilluminating configuration for observation of fluorescence resonance energy transfer (FRET) (Tsien and Miyawaki, 1998; Harpur and Bastiaens, 2000) to monitor both the translocation of MARCKS and its association with Ca^{2+}-CaM.

MATERIALS AND METHODS

Epiilluminating set up

A glass plate with a refractive index of 1.51633 (OHARA, S-BSL7) had an antireflection coat on the reverse side, allowing 4 to 5% of incident light to be reflected by the front side of the glass. Transmittance of the glass was measured using a spectrophotometer (Hitachi U-3310, Tokyo, Japan). The glass plate was mounted in a normal or the specific filter cube. In the latter case, the cube was inserted below the stage of an inverted microscope (IX70, Olympus, Tokyo, Japan), in place of the turret containing normal filter cubes (Fig. 1 *C*).

Gene construction

PKCγ-DsRed was purchased from CLONTECH Laboratories (Palo Alto, CA) (pPKCγ-DsRed1). The creation of MARCKS-GFP has been described previously (Ohmori et al., 2000). The GFP gene of the MARCKS-GFP construct was replaced with the gene of a less pH-sensitive yellow fluorescent protein (YFP) (EYFP-V68L/Q69K) (Miyawaki et al., 1999) to construct MARCKS-YFP. The cDNAs of CFP-CaM (Miyawaki et al., 1997), Sapphire-pm, YFP-mt, DsRed-nu were cloned into the *Hin*dIII and *Eco*RI sites of the pcDNA3 vector (Invitrogen, Carlsbad, CA). We created Sapphire-pm by extending Sapphire cDNA at the 5′ end with a sequence encoding the 22 N-terminal amino acids of the nonreceptor tyrosine kinase, Lyn. The 12 N-terminal amino acids of the cytochrome *c* oxidase subunit IV presequence or the nuclear localization signal (MPKKKRKVEDA) were fused to the N-termini of EYFP-V68L/Q69K and DsRed to obtain YFP-mt and DsRed-nu, respectively.

Imaging

HeLa cells were grown on a 35-mm glass-bottom dish in Dulbecco's modified Eagle's medium containing 10% fetal bovine serum. Cells were imaged 2 to 5 days after cDNA transfection with lipofectin (Life Technologies/Gibco-BRL, Gaithersburg, MD). The concentration of fetal bovine serum was reduced to 0.2% for half a day before imaging. Cells were imaged on an inverted microscope (Olympus IX70) with a standard 75-W xenon lamp and a 40× objective lens (Uapo/340, N.A. 1.35). For Ca^{2+} imaging using fura-2, cells were loaded with the dye before visualization. Interference filters (excitation and emission filters) contained in wheels, were automated using Lambda 10–2 hardware (Sutter Instruments, Novato, CA). The filter-switching time was set to 50 ms. With this setting, the speed for obtaining the signals at each cycle can be maximized to 2 Hz for triple- and 4 Hz for dual-color imaging. The neutral density (ND) filters, interference filters, and reflectors used in the experiments are listed in Tables 1 and 2. Emitted light was captured by a cooled CCD camera (Cool Snap fx, Roper Scientific, Tucson, AZ). The whole system was controlled using the MetaFluor 4.5 software (Universal Imaging, Media, PA).

RESULTS AND DISCUSSION

Novel epiilluminating system using a glass reflector

We invented a power meter capable of measuring the power density (W/cm^2) of excitation light at the specimen level on an inverted epifluorescence microscope (manuscript in preparation). By optimizing the intensity of excitation light with the power meter, we have realized that only a small amount of light from a 75-W xenon lamp is required for fluorescence imaging in living cells. For example, yellow cameleons are genetically encoded fluorescent Ca^{2+} indicators structurally based on CaM (Miyawaki et al., 1997, 1999), CFP, and YFP (cyan- and yellow-variants of GFP, respectively) (for review, see Tsien, 1998). Intense illumination affects the baseline Ca^{2+} signal (the emission ratio of yellow/cyan), as seen in Fig. 1 *A*. For a sampling interval of 4 s, the light from a 75-W xenon lamp should be reduced to 3% or less by inserting ND filters in the epiilluminating light path. Without this attenuation, the photochromism of YFP (Tsien, 1998) caused the baselines to decrease gradually. This weak illumination was sufficient to obtain bright fluorescence images of yellow cameleons. A 75-W xenon lamp aimed through ordinary optics also puts out enough energy for fura-2 measurements, allowing the illumination light to be reduced to 1 to 5%.

To discard most of the light, while sending a small fraction to the sample, we replaced the ordinary dichroic mirror with a glass plate, which exhibits >90% transmittance in a wide range of 350 to 650 nm (Fig. 1 *B*). This configuration permitted the detection of fluorescent dyes with the appropriate excitation and emission filters (Fig. 1 *C*) without the need for a rigorous attenuation of excitation light using ND filters. One concern was that an important amount of the light passing through the glass entered the observation light path. To eliminate background illumination, we developed a specific filter cube effectively deflecting the passing light out of the microscope with a mirror (Fig. 1 *C*). Although the specific cube was used in the present study, it is not always necessary. The glass plate mounted in a normal cube can be used (see Fig. 5) as long as the transmission ranges of the excitation and emission

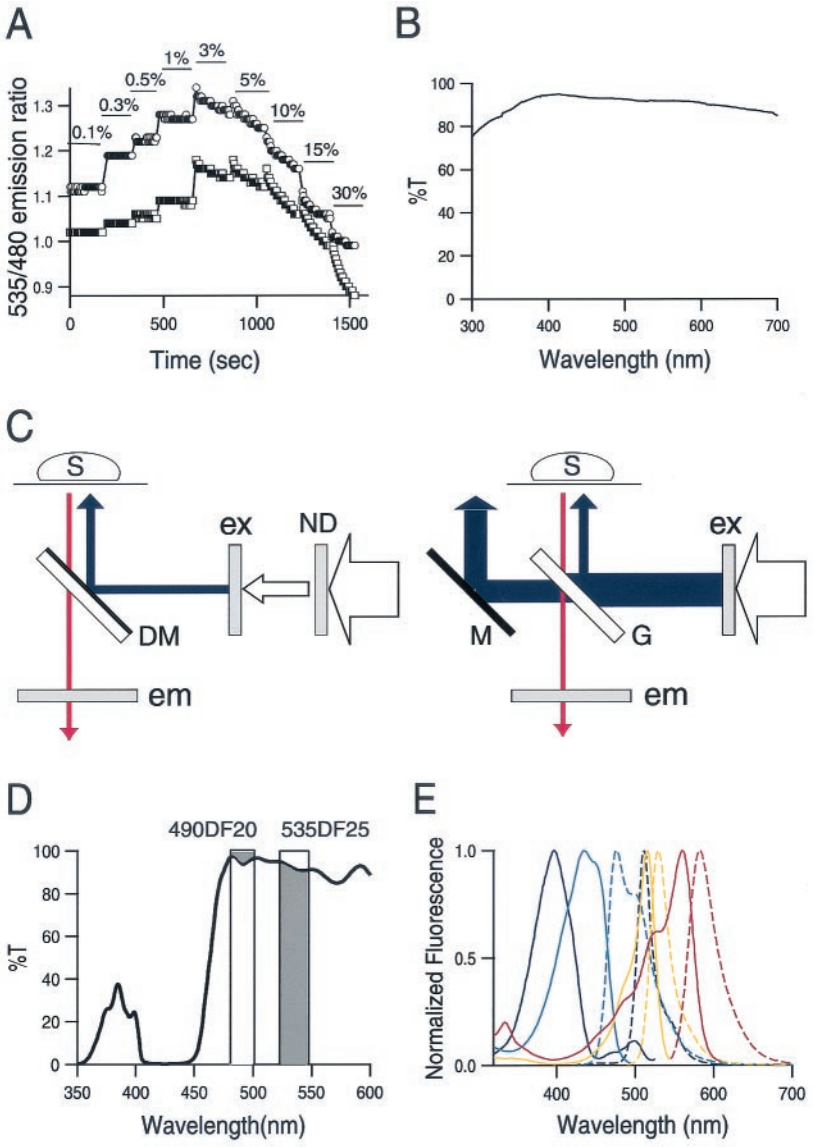

FIGURE 1 Reflectors for epifluorescence microscopy. (*A*) Ratios of yellow cameleon-2.1 (Miyawaki et al., 1999) emissions at 535 to 480 nm in two resting HeLa cells illuminated by a 75-W xenon lamp. The excitation light was attenuated using ND filters (the extent of the attenuation is indicated in the graph). In the epiilluminating configuration with 440DF20 and 455DRLP (see Table 1), the power density of excitation light at the cell level was measured ~3 W/cm^2 without ND filters. (*B*) Transmission curve of the glass with a refractive index of 1.51633 (S-BSL7, OHARA) having an antireflection coat on the reverse side. It allows 4 to 5% of incident light to be reflected by the front side. The transmission at wavelengths below 400 nm is slightly decreased due to absorption of the incident light by the glass. (*C*) Epifluorescence microscopes with a highly reflective reflector (*left*, a conventional epiillumination system) and a nonreflective reflector (*right*, our novel epiillumination system). Excitation and emission light paths are drawn in blue and red, respectively. The glass plate was mounted in the specific filter cube, which was inserted below the stage of an inverted microscope in place of a turret. ex, Excitation filter; em, emission filter; DM, dichroic mirror; G, glass; M, mirror; S, sample. (*D*) Novel way of using a normal dichroic mirror. The transmission curve of 455DRLP is shown. Boxes indicate the passbands of the excitation filter (490DF20) and the emission filter (535DF25) used for direct excitation of MARCKS-YFP. Reflection present between 480 and 500 nm and the transmission occurring between 522.5 and 547.5 nm are indicated in gray. (*E*) The excitation (*solid lines*) and emission (*dotted lines*) spectra of Sapphire, CFP, YFP, and DsRed used for the 4-fluorophore imaging. They are drawn in violet, cyan, yellow, and red, respectively.

filters are well separated with high blocking efficiency. The filters listed in Tables 1 and 2 have been shown to have high blocking efficiency in the nontransmission regions. The use of the normal filter cube should augment applicability of our imaging system, because it proved to block effectively a large amount of the excitation light passing through the glass (see Fig. 5), and because a standard microscope is equipped with the cube. Also when more than 5% of incoming light is necessary for exciting samples, another glass plate that shows ~10% reflection and 90% transmittance

TABLE 1 Optical components used in experiments of Figs. 1A, 2, 3, and 4

Exp.	Dye		ND Filter*	Filter in the Wheel/Excitation Light Path†	Reflector	Filter in the Wheel/Emission Light Path†
Fig. 1A	Yellow cameleon 2.1	Donor channel FRET channel	Indicated in the graph	440DF20	455DRLP	480DF30 (200 ms) 535DF25 (200 ms)
Figs. 2 and 3	Fura-2		———	340HT15 (20 ms) 380HT15 (10 ms)	glass‡	535DF25
	MARCKS-GFP			490DF20		535DF25 (50 ms)
	PKCγ-DsRed			546DF10		595RDF60 (100 ms)
Fig. 4	CFP-CaM & MARCKS-YFP	Donor channel FRET channel	———	1% ND & 440DF20	455DRLP	480DF30 (200 ms) 535DF25 (200 ms)
	MARCKS-YFP (acceptor channel)		———	490DF20		535DF25 (200 ms)

*ND filters in the holder of the illuminator.
†DF, RDF, and HT represent band-pass filters. The first number gives the center of the passband and the second number designates the full width at half-maximal transmission. The camera exposure time is indicated between parentheses.
‡The glass plate was mounted in the specific cube; otherwise the relfectors were placed in normal cubes.

can be used. Its performance for the multicolor imaging has also been verified (data not shown).

Simultaneous imaging of $[Ca^{2+}]_i$, redistributions of PKCγ and MARCKS

To monitor the translocation of MARCKS together with the two upstream signals, Ca^{2+} and membrane-associated PKC activity, in single live cells, we used a GFP-conjugated MARCKS (MARCKS-GFP) (Ohmori et al., 2000) and a red fluorescent protein-conjugated PKCγ (PKCγ-DsRed, CLONTECH). Although translocation of PKCγ to the plasma membrane does not ensure its activation, this step is required for phosphorylation of MARCKS on the membranes (Oancea et al., 1998; Ohmori et al., 2000). For the measurement of $[Ca^{2+}]_i$, fura-2 was used.

In the present study, we induced Ca^{2+} and PKC signals through receptor-activation, instead of applying ionomycin (Ca^{2+} ionophore) and phorbol-ester. Treatment of HeLa cells with ATP and EGF (epidermal growth factor) activates

TABLE 2 Optical components used for a 4-fluorophore imaging (Fig. 5)

Picture	Dye	ND Filter*	Filter in the Wheel/Excitation Light Path	Reflector	Filter in the Wheel/Emission Light Path
A	Sapphire-pm	10% ND	400DF15	505DRLPXR†	535DF25
B	CFP-CaM		440DF20	455DRLP	480DF30
C	YFP-mt		490DF20	505DRLPXR†	535DF25
D	DsRed-nu		546DF10	560DRLP	595RDF60
E	Sapphire-pm	———	400DF15	Glass‡	535DF25
F	CFP-CaM		440DF20		480DF30
G	YFP-mt		490DF20		535DF25
H	DsRed-nu		546DF10		595RDF60
I	Sapphire-pm	———	400DF15	Glass	535DF25
J	CFP-CaM		440DF20		480DF30
K	YFP-mt		490DF20		535DF25
L	DsRed-nu		546DF10		595RDF60
M	Sapphire-pm	———	10% ND & 400DF15	455DRLP	535DF25
N	CFP-CaM		10% ND & 440DF20		480DF30
O	YFP-mt		490DF20		535DF25
P	DsRed-nu		546DF10		595RDF60

*ND filters in the holder of the illuminator.
†DRLPXR represents a long-pass dichroic mirror with a wide range of reflection.
‡The glass plate in the specific cube.

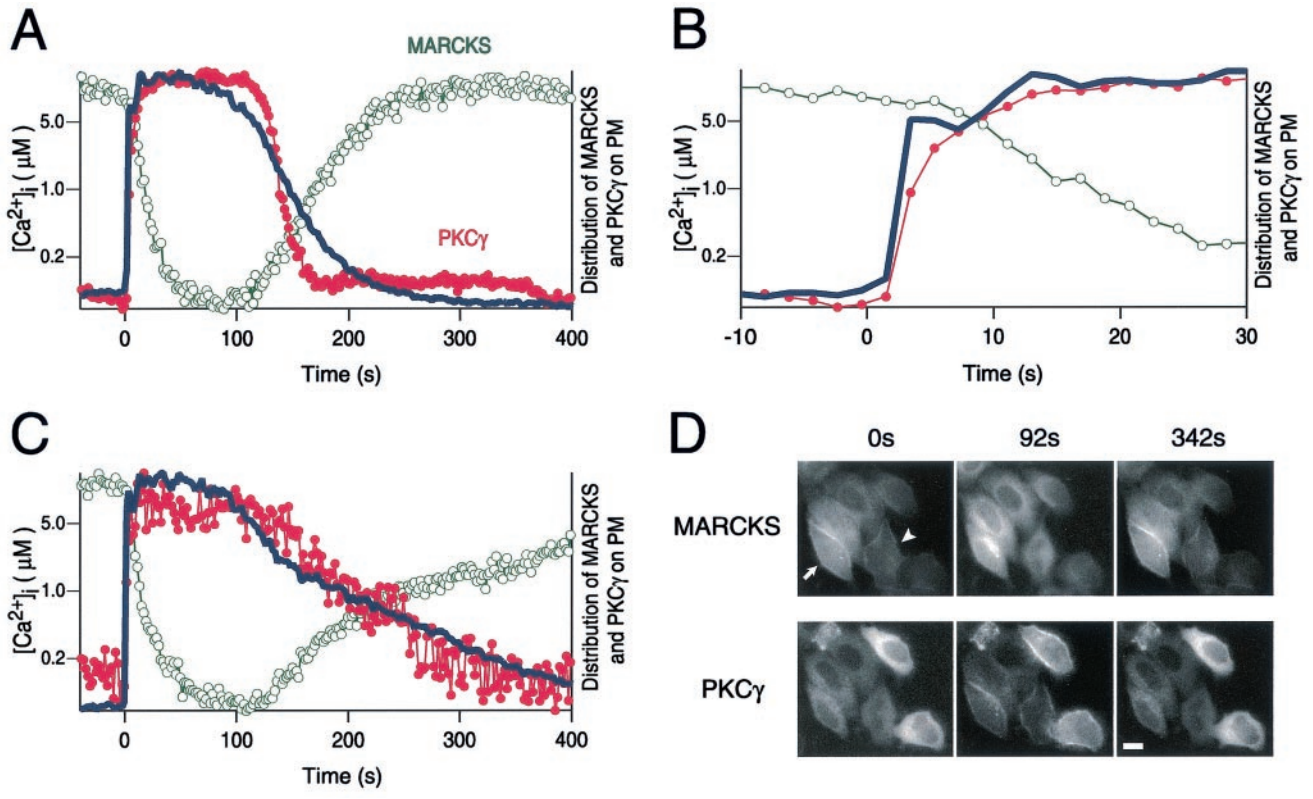

FIGURE 2 Simultaneous imaging of $[Ca^{2+}]_i$, PKC and MARCKS. HeLa cells were transfected with 0.2 μg/dish of MARCKS-GFP/pcDNA3 and 2 μg/dish of PKCγ-DsRed/pcDNA3. (*A*) Temporal profiles of distribution of MARCKS-GFP (*green open circles*) and PKCγ-DsRed (*red closed circles*), and $[Ca^{2+}]_i$ (*blue line*) in a single HeLa cell (indicated by an *arrow* in *D*), following the stimulation with 10 μM ATP. To determine the distribution of MARCKS-GFP and PKCγ-DsRed on the plasma membrane, the relative fluorescence intensity in a region of the plasma membrane was calculated in comparison to the cytosol as previously described (Oancea and Meyer, 1998). The left-hand ordinate calibrates $[Ca^{2+}]_i$ in μM. (*B*) The initial responses of the signals in Fig. 2 *A* are shown on an expanded time scale. (*C*) Temporal profiles of distribution of MARCKS-GFP (*green open circles*) and PKCγ-DsRed (*red closed circles*), and $[Ca^{2+}]_i$ (*blue line*) obtained from another HeLa cell (indicated by an *arrowhead* in *D*). (*D*) The fluorescence images of MARCKS-GFP (exposure time, 50 ms) and PKCγ-DsRed (exposure time, 100 ms) were taken at 0, 92, and 342 s after stimulation with 10 μM ATP. Scale bar = 10 μm.

phospholipase Cβ (PLCβ) and phospholipase Cγ (PLCγ), respectively. Both signals cause the hydrolysis of phospholipids, leading to the activation of both the inositol-1,4,5-trisphosphate/Ca^{2+} and diacylglycerol/PKC pathways. Fig. 2 *A* details the temporal profiles of $[Ca^{2+}]_i$ (blue line) as well as redistribution of PKCγ (red closed circles) and MARCKS (green open circles) in one of six HeLa cells shown in Fig. 2 *D* (indicated by an arrow). Activation of PLCβ with 10 μM ATP produced a rapid increase in $[Ca^{2+}]_i$, followed by a plateau. $[Ca^{2+}]_i$ then gradually returned to the previous resting level. Translocation of PKCγ was nicely synchronized with the Ca^{2+} transient, illustrating the $[Ca^{2+}]_i$ sensing ability of the C2-domain of PKCγ (Oancea and Meyer, 1998). Translocation of MARCKS occurred gradually, but on the whole, in a reciprocal manner to PKCγ. Fig. 2 *B* expands the initial phase of Fig. 2 *A*. The use of the epiillumination system containing the nonreflective glass plate allowed the measurement of each signal every 1 to 2 s. The $[Ca^{2+}]_i$ rise was immediately followed by the translocation of PKCγ, whereas MARCKS started to translocate with a latent time of ~4 s. Although each of the signals showed the same onset in all of the six HeLa cells, there was heterogeneity in the returning phase. Fig. 2 *C* shows the temporal profiles of the three signals that returned more slowly in another HeLa cell (indicated by an arrowhead in Fig. 2 *D*).

However, activation of PLCγ with 10 ng/ml EGF resulted in a hardly detectable change in $[Ca^{2+}]_i$ with significant translocations of both PKCγ and MARCKS (Fig. 3). Subsequent activation of PLCβ with 10 μM ATP provoked the mobilization of Ca^{2+} from intracellular stores, and trafficking of PKCγ and MARCKS, similar to those shown in Fig. 2. Although it is difficult to quantify the translocation of PKCγ and MARCKS, fura-2 measurement of Ca^{2+} is relatively quantitative. It was evident from our measurements that the amount of the mobilized Ca^{2+} differed substantially between the PLCβ and PLCγ stimulations. It seemed that the binding of Ca^{2+}-CaM complexes resulting from the activation of PLCβ contributed to MARCKS translocation, whereas only PKC worked on MARCKS when

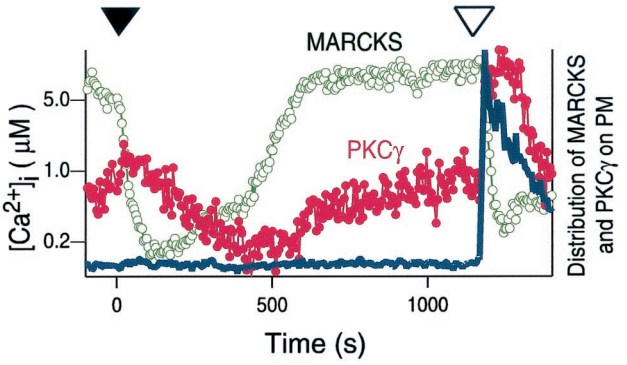

FIGURE 3 Simultaneous imaging of $[Ca^{2+}]_i$, PKC, and MARCKS in a HeLa cell stimulated with 10 ng/ml EGF (*filled arrowhead*) followed by 10 μM ATP (*open arrowhead*). HeLa cells were transfected with 0.2 μg/dish of MARCKS-GFP/pcDNA3 and 2 μg/dish of PKCγ-DsRed/pcDNA3. Data points of the distribution of MARCKS-GFP (*green open circles*), PKCγ-DsRed (*red filled circles*), and $[Ca^{2+}]_i$ (*blue line*) are plotted as in Fig. 2.

PLCγ was activated. Although there is a consensus that the phosphorylation of MARCKS by PKC is important in the regulation of MARCKS translocation (Kim et al., 1994; Ohmori et al., 2000), there is no direct evidence in live cells for the involvement of Ca^{2+}-CaM binding in this process. To observe the contribution of Ca^{2+}-CaM alone, we used inhibitors for PKC in conjunction with PLCβ activation. The results, however, were ambiguous; ATP-induced translocation of MARCKS-GFP was blocked when cells were treated with 1 μM staurosporine (results not shown) but not blocked with 0.1 μM staurosporine or 5 μM bisindolylmaleimide, GF 109203X (Toullec et al., 1991) (Fig. 4 *B*, top). Treatment with 1 μM staurosporine greatly changed the cell morphology, suggesting some nonspecific effects. Assuming that PKC activity in HeLa cells was fully inhibited by 0.1 μM staurosporine or 5 μM GF 109203X, these results indicated that the translocation of MARCKS could be caused by some other mechanisms than its phosphorylation by PKC, possibly the interaction with Ca^{2+}-CaM.

Direct observation of physical interaction between MARCKS and Ca^{2+}-CaM

To directly observe the interaction between MARCKS and Ca^{2+}-CaM, we expressed two chimeric proteins, MARCKS-YFP and CFP-CaM, in HeLa cells and measured the FRET between CFP and YFP (Miyawaki and Tsien, 2000). In experiments to observe intermolecular FRET, donor and acceptor molecules move independently before they associate. Thus, the stoichiometry of acceptors to donors could vary spatially and temporally. This is the case with our experiment: MARCKS-YFP translocated from the plasma membrane to cytosol after stimulation. We therefore took the following two approaches.

First, because calculation of the simple emission ratio of YFP to CFP does not give reliable information about the interaction between MARCKS and CaM, we performed the acceptor (YFP) bleaching (Bastiaens et al., 1996; Miyawaki and Tsien, 2000; Harpur and Bastiaens, 2000). This internal calibration approach allowed us to quantify the interaction of MARCKS-YFP in the cytosol with CFP-CaM. A general filter set was used for the measurement of FRET between CFP and YFP: a 440DF20 excitation filter, a 455DRLP dichroic mirror, and two emission filters (480DF30 for the donor channel monitoring CFP; 535DF25 for the FRET channel monitoring YFP) alternated by a filter changer. In contrast to intensity-based ratiometric imaging, measurement of the fluorescence lifetime of the donor (CFP) with FLIM (fluorescence lifetime imaging microscopy) should allow to obtain a continuous and internally calibrated quantification of FRET efficiency (Harpur and Bastiaens, 2000; Harpur et al., 2001).

Second, along with the FRET observation, we monitored the translocation of MARCKS-YFP by direct excitation of YFP. Monitoring of YFP usually uses a 490DF20 excitation filter, a 505DRLP dichroic mirror, and a 535DF25 emission filter (acceptor channel). With a conventional imaging system, therefore, the dichroic mirrors must be exchanged manually or automatically between the 455DRLP and 505DRLP for simultaneous observation of the FRET and MARCKS translocation. This lowers imaging performance. In addition, multichroic mirrors are of no use for the simultaneous observation, because the excitation band (490DF20) of the acceptor channel and the emission band (480DF30) of the donor channel are in conflict. On the other hand, our imaging system using the glass plate allows the simultaneous observation of FRET and acceptor molecules without changing the reflectors, because it works irrespective of the colors of fluorophores. We also evaluated an alternative configuration using a single, commercially available dichroic mirror instead of the glass plate. A 455DRLP was mounted in a normal filter cube. As shown in Fig. 1 *D*, 5% of the total light at 490 nm, reflected by the 455DRLP dichroic mirror, was used for the direct excitation of YFP. In contrast, illumination at 440 nm was reduced by placing an ND filter (1% transmission) over the 440DF20 excitation filter in the filter exchanger (Table 1). This configuration is substantially equal to the configuration with the glass plate, in that both use highly light-transmissive reflectors, enabling us to monitor the three signals through the donor, FRET, and acceptor channels without changing the reflectors (Table 1).

Fig. 4 shows the signals of MARCKS-YFP on the cytosol and membrane, through the acceptor channel (top panels), as well as signals through the donor and FRET channels (middle panels). They reflect the MARCKS translocation and its interaction with CaM, respectively. While the cytosolic distribution of MARCKS was detected, YFP was bleached out by illuminating the specimen through a

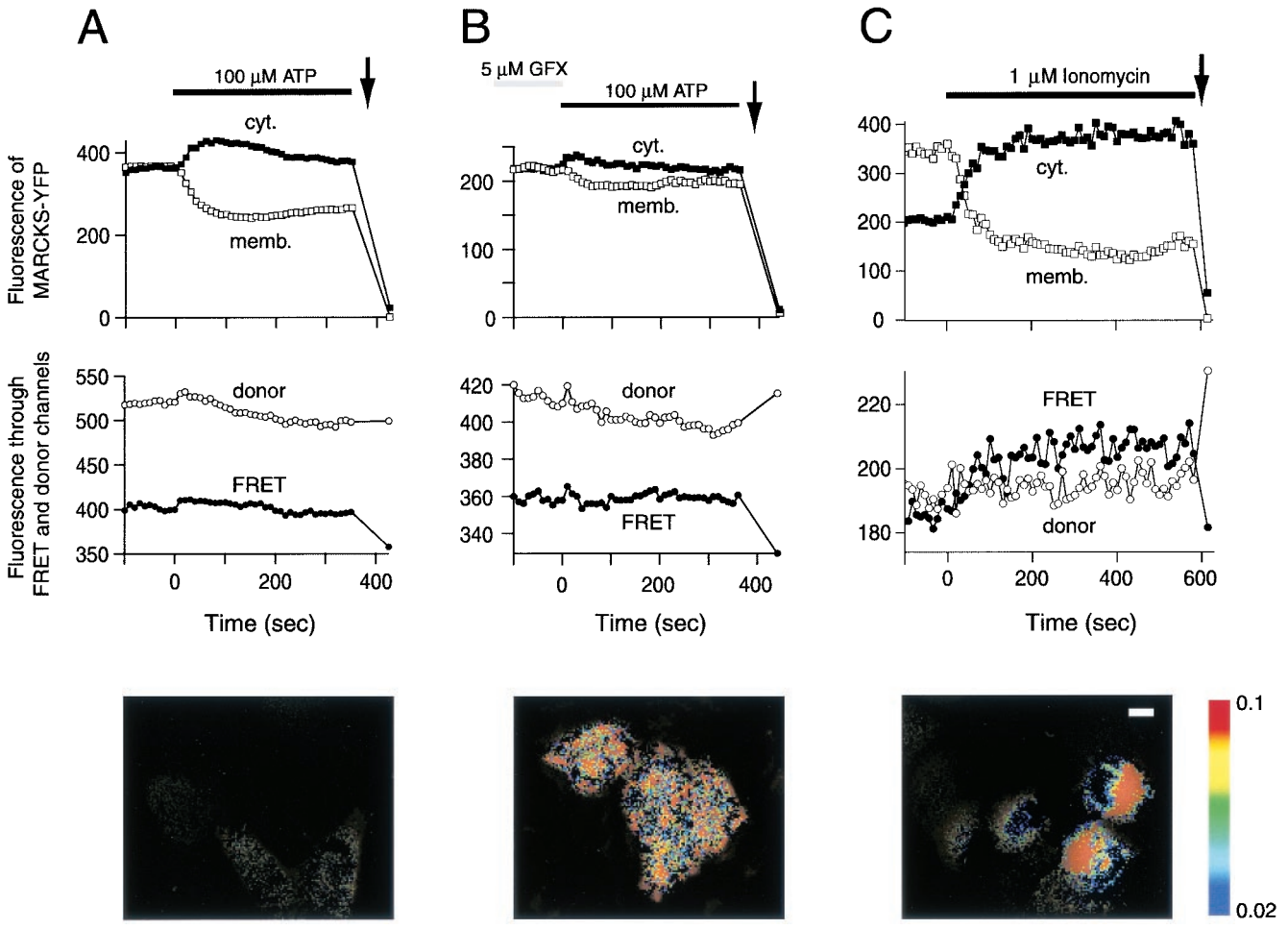

FIGURE 4 Interaction of MARCKS with Ca^{2+}-CaM in the cytosol of single HeLa cells. HeLa cells were transfected with 0.3 μg/dish of MARCKS-YFP/pcDNA3 and 0.03 μg/dish of CFP-CaM/pcDNA3. Cells were treated with 100 μM ATP (*A*), 5 μM GF 109203X followed by 100 μM ATP (*B*), and 1 μM ionomycin (*C*). (*Top*) Monitoring of the translocation of MARCKS by direct excitation of MARCKS-YFP using a 455DRLP dichroic mirror. The fluorescence intensities through the novel acceptor channel (Fig. 1 *D*) of the plasma membrane (*open squares*) and cytosol (*filled squares*) are plotted. (*Middle*) Monitoring of the interaction between MARCKS and Ca^{2+}-CaM in the cytosol by measuring the FRET from CFP to YFP. FRET was detected by the dequenching of CFP following bleaching of YFP. Temporal profiles of emission signals through donor (*open circles*) and FRET (*filled circles*) channels are shown. The acceptor bleaching was completed within 10 to 20 s. The complete bleaching of YFP was confirmed by the fact that the fluorescence through the acceptor channel dropped to almost zero (*top*). The time points of the YFP bleaching are indicated by arrows. (*Bottom*) Pseudo-color map of FRET efficiency based on the YFP bleaching. The ratio of the increase in CFP fluorescence signal to its post-bleach signal is represented as reported previously (Bastiaens et al., 1996). Scale bar = 10 μm.

525DF45 excitation filter and a 560DRLP dichroic mirror. The increase in the signal through donor channel after the bleaching was imaged (bottom panels) as reported previously (Bastiaens et al., 1996). After stimulation with 100 μM ATP, which caused long-lasting redistribution of MARCKS, bleaching of YFP did not dequench the CFP fluorescence (Fig. 4 *A*). Dequenching of CFP was not seen in cells stimulated by EGF either (data not shown). In contrast, when cells were pretreated with 5 μM GF 109203X to block PKC activation, the emission of CFP increased in the membrane region as well as in the cytosolic fraction upon YFP-bleaching (Fig. 4 *B*, middle and bottom), indicating FRET between CFP and YFP. This result demonstrates the presence of physical interaction between MARCKS-YFP and CFP-CaM. The dependency of FRET on the PKC-blockade (GF 109203X) was observed reproducibly with an earlier execution of YFP-bleaching (data not shown). A significant translocation of MARCKS-YFP and cytosolic FRET were also observed following treatment with 1 μM ionomycin (Fig. 4 *C*) or with 1 μM thapsigargin (data not shown). Only in experiments where Ca^{2+}-mobilization artificially predominates PKC activation, the FRET was positively detected. These findings suggest that physiological receptor-activation leading to the hydrolysis of phospholipids provokes the translocation of MARCKS, principally through the activation of a PKC signal. On the

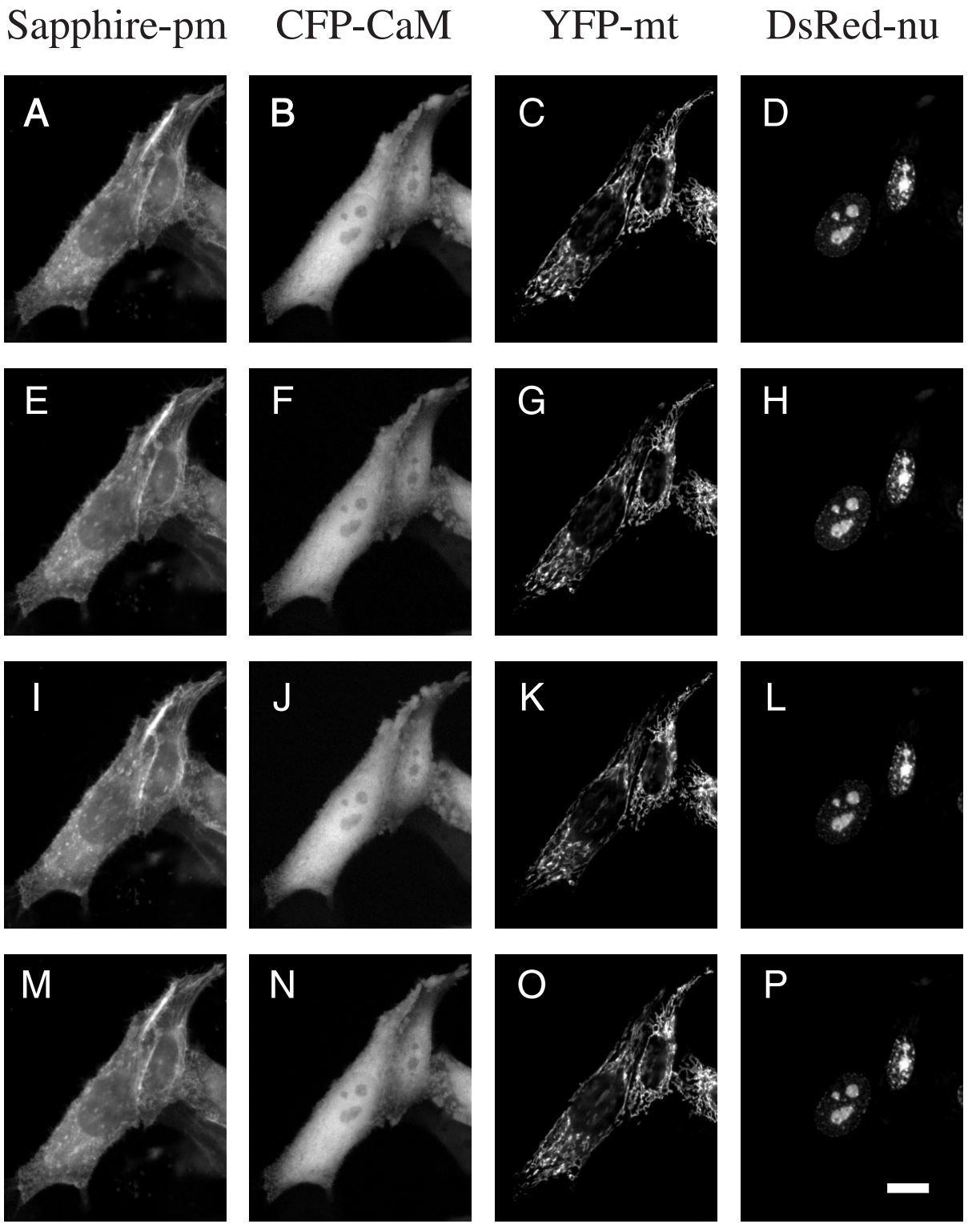

FIGURE 5 Simultaneous imaging of Sapphire, CFP, YFP, and RFP. HeLa cells were imaged for Sapphire-pm (A, E, I, and M), CFP-CaM (B, F, J, and N), YFP-mt (C, G, K, and O), and DsRed-nu (D, H, L, and P). The images were obtained using either the appropriate dichroic mirrors (*A–D*), the glass plate in the specific cube (*E–H*), the glass plate in a normal cube (*I–L*), or a 455DRLP in a normal cube (*M–P*). The excitation and emission filters, reflectors, and ND filters are shown in Table 2. Scale bar in $P = 10\ \mu$m.

other hand, physiological predominance of Ca^{2+}-mobilization over PKC activation could be seen in excitable cells such as neurons, during depolarization and firing. The interaction between MARCKS and CaM is now under investigation in dissociated hippocampal neurons when they are pharmacologically depolarized.

Simultaneous 4-fluorophore imaging of subcellular structures

The generation of spectral mutants of GFP and the cloning of genes encoding RFPs prompted us to label living cells with as many spectrally different dyes as possible. To prove the validity of our new imaging system, we tried a labeling of subcellular structures in living cells with four different fluorophores. We constructed four chimeric proteins using DsRed (CLONTECH) and the three *Aequorea* GFP mutants, Sapphire (=H9) (Tsien, 1998), CFP, and YFP (excitation and emission spectra are shown in Fig. 1 *E*). With the appropriate targeting signals, Sapphire, YFP, and DsRed were localized to the plasma membrane (Sapphire-pm), mitochondria (YFP-mt), and nucleus (DsRed-nu), respectively; CFP was fused to CaM (CFP-CaM). Two days after co-transfection, HeLa cells expressing all four chimeric proteins were visualized. Attenuation of the illumination light with a 10% ND transmission filter and four normal cubes containing the appropriate excitation and emission filters and dichroic mirrors (Table 2) gave four distinct images (Fig. 5, *A–D*), showing differential targeting of the four fluorescent proteins. Then the specific cube accommodating the glass plate was substituted. Only exchanging excitation and emission filters (Table 2) allowed us to obtain four images (Fig. 5, *E–H*), equal to or slightly brighter than Fig. 5 (*A–D*), respectively. It appears that the light emitted from the cells was efficiently directed to detectors, as the glass transmits ~96% of the light. Next, another set of pictures (Fig. 5, *I–L*) was obtained using the glass plate placed in a normal cube. In terms of image contrast, there is no difference between the two sets of pictures (Fig. 5, *E–H* and *I–L*), indicating that the specific cube is not absolutely necessary. Finally, a commercially available dichroic mirror in a normal cube was used. We chose 455DRLP for its high transmittance with respect to the fluorescence of all four fluorescent proteins (as can be seen by comparing the transmission curve in Fig. 1 *D* with the dotted lines in Fig. 1 *E*). ND filters (10% transmission) were placed over the 400DF15 and 440DF20 filters inside the wheel for the excitation of Sapphire and CFP, respectively (Table 2). This set-up gave images shown in Fig. 5, *M–P*, which are comparable with the others. The availability of a single commercial dichroic mirror further demonstrates the easy applicability of our technique. It should be noted that the speed of sequential acquisition of the four pictures could be significantly increased by the use of single reflectors (Fig. 5, *E–P*).

Simultaneous detection of multiple GFP variants in living cells has also been carried out by FLIM (Pepperkok et al., 1999). Although FLIM is not easily implemented by most investigators due to the requirement of specialized equipment and expertise, it is particularly powerful for discrimination of spectrally similar fluorophores (Harpur et al., 2001), because the readout requires only a single dichroic mirror and an emission filter. By contrast, our new technique is applicable to full range of spectral variation. We demonstrate the easy access of this approach in the case of four fluorophore imaging of spectrally distinct fluorescent proteins with a conventional fluorescence microscope only containing a single reflector.

CONCLUSION

For fluorescence imaging of living cells, it is important 1) to reduce the intensity of illumination light to minimize photodamage of samples and photobleaching of fluorophores, and 2) to maximize the efficiency for collecting emitted fluorescence for better signal-to-noise ratio of images. Based on these two principles, our novel imaging system uses a reflector that shows a high light transmittance in a wide range of wavelength, providing a powerful technique for multicolor imaging with the following advantages.

The first advantage is that it is flexible and broadly applicable. The system is applicable to any set of fluorophores, allowing, for instance, the simultaneous monitoring of FRET and acceptor molecules (Fig. 4), or the 3-fluorophore imaging of fura-2, GFP, and RFP (Figs. 2 and 3). Neither could be performed using multichroic mirrors. Our system also permits the 4-fluorophore imaging of Sapphire, CFP, YFP, and RFP (Fig. 5). By contrast, most studies by conventional multicolor imaging of live cells use only two fluorophores (dual-color) or limited sets of dyes.

The second advantage is that it is reasonably fast (up to 2 Hz for triple-, and 4 Hz for dual-color imaging). Without the need for changing reflectors, multiple images can be obtained fast enough to follow cellular dynamics that occurs on the order of seconds, such as Ca^{2+} and Ca^{2+}-related events.

The third advantage is that it is readily applicable and economical. Our new system requires no highly specialized equipment or expertise for implementation. The cost for the glass plate is very low. Also we present a new way for using a single commercial dichroic mirror for simultaneous imaging of multiple fluorophores.

Since many spectral variants of GFP and RFP have emerged, more and more investigators are interested in simultaneous imaging of multiple fluorophores and FRET analysis. Our novel imaging system should popularize these technologies and help clarify the dynamic interactions of proteins and subcellular structures in living cells.

The authors thank Drs. K. Abe, K. Osa, K. Kawano, and S. Shimizu for valuable advice, Drs. R.Y. Tsien, D. Zacharias, and C. Zuker for critical reading of the manuscript. This work was partly supported by grants from CREST (the Japan Science and Technology Corporation), the Japanese Ministry of Education, Science and Culture.

REFERENCES

Bastiaens, P. I., I. V. Majoul, P. J. Verveer, H. D. Soling, and T. M. Jovin. 1996. Imaging the intracellular trafficking and state of the AB5 quaternary structure of cholera toxin. *EMBO J.* 15:4246–4253.

Blackshear, P. J. 1993. The MARCKS family of cellular protein kinase C substrates. *J. Biol. Chem.* 268:1501–1504.

Chakravarthy, B. R., R. J. Isaacs, P. Morley, J. P. Durkin, and J. F. Whitfield. 1995a. Stimulation of protein kinase C during Ca^{2+}-induced keratinocyte differentiation. *J. Biol. Chem.* 270:1362–1368.

Chakravarthy, B. R., R. J. Isaacs, P. Morley, and J. F. Whitfield. 1995b. Ca^{2+} -calmodulin prevents myristoylated alanine-rich kinase C substrate protein phosphorylation by protein kinase Cs in C6 rat glioma cells. *J. Biol. Chem.* 270:24911–24916.

Chakravarthy, B. R., P. Morley, and J. F. Whitfield. 1999. Ca^{2+}-calmodulin and protein kinase Cs: a hypothetical synthesis of their conflicting convergences on shared substrate domains. *Trends Neurosci.* 22:12–16.

Graff, J. M., T. N. Young, J. D. Johnson, and P. J. Blackshear. 1989. Phosphorylation-regulated calmodulin binding to a prominent cellular substrate for protein kinase C. *J. Biol. Chem.* 264: 21818–21823.

Harpur, A. G., and P. I. H. Bastiaens. 2000. Probing protein interactions using GFP and fluorescence resonance energy transfer. *In* The Molecular Cloning. J. Sambrook and D. W. Russell, editors. Cold Spring Harbor Laboratory Press, Cold Spring Harbor, NY. 18.69–18.95.

Harpur, A. G., F. S. Wouters, and P. I. H. Bastiaens. 2001. Imaging FRET between spectrally similar GFP molecules in single cells. *Nat. Biotechnol.* 19:167–169.

Kim, J., T. Shishido, X. Jiang, A. Aderem, and S. McLaughlin. 1994. Phosphorylation, high ionic strength, and calmodulin reverse the binding of MARCKS to phospholipid vesicles. *J. Biol. Chem.* 269: 28214–28219.

Miyawaki, A., O. Griesbeck, R. Heim, and R. Y. Tsien. 1999. Dynamic and quantitative Ca^{2+} measurements using improved cameleons. *Proc. Natl. Acad. Sci. U. S. A.* 96:2135–2140.

Miyawaki, A., J. Llopis, R. Heim, J. M. McCaffery, J. A. Adams, M. Ikura, and R. Y. Tsien. 1997. Fluorescent indicators for Ca^{2+} based on green fluorescent proteins and calmodulin. *Nature.* 388:882–887.

Miyawaki, A., and R. Y. Tsien. 2000. Monitoring protein conformations and interactions by fluorescence resonance energy transfer between mutants of green fluorescent protein. *Methods Enzymol.* 327:472–500.

Oancea, E., and T. Meyer. 1998. Protein kinase C as a molecular machine for decoding calcium and diacylglycerol signals. *Cell.* 95:307–318.

Ohmori, S., N. Sakai, Y. Shirai, H. Yamamoto, E. Miyamoto, N. Shimizu, and N. Saito. 2000. Importance of protein kinase C targeting for the phosphorylation of its substrate, myristoylated alanine-rich C-kinase substrate. *J. Biol. Chem.* 275:26449–26457.

Pepperkok, R., A. Squire, S. Geley, and P. I. H. Bastiaens. 1999. Simultaneous detection of multiple green fluorescent proteins in live cells by fluorescence lifetime imaging microscopy. *Curr. Biol.* 9:269–272.

Toullec, D., P. Pianetti, H. Coste, P. Bellevergue, T. Grand-Perret, M. Ajakane, V. Baudet, P. Boissin, E. Boursier, F. Loriolle, L. Duhamel, D. Charon, and J. Kirilovsky. 1991. The bisindolylmaleimide GF 109203X is a potent and selective inhibitor of protein kinase C. *J. Biol. Chem.* 266:15771–15781.

Tsien, R. Y. 1998. The green fluorescent protein. *Annu. Rev. Biochem.* 67:509–544.

Tsien, R. Y., and A. Miyawaki. 1998. Seeing the machinery of live cells. *Science.* 280:1954–1955.